Department of Environment System

Graduate School of Frontier Sciences

The University of Tokyo

2021

Master's Thesis

Numerical simulation of indoor airflow field using air curtain jet (ACJ) ventilation mode —Analysis of the thermal environment with different heat source conditions

Submitted February 28, 2022

Adviser: Assistant Professor, Masaatsu AICHI

Feilula Haishaer

菲露拉 海沙尔

Acknowledgement

Upon the completion of this thesis, I would like to thank the many people who have helped and encouraged me.

First of all, I would like to thank my supervisor Assistant Professor Masaatsu AICHI, for his generous advice and patient guidance during these two and a half years, as well as the support of my ideas and tolerance of my shortcomings when I encountered problems. Thank you from the bottom of my heart. I would also like to thank my sub-supervisor Assistant Professor Makoto Akizuki for giving me very professional advice during the discussion of my research.

In addition, I would like to thank my lab mates, for your company and support, I have spent a very happy and memorable time.

Finally, I would also like to thank my family for their unconditional support and love, thank you for accompanying me through every tough moment.

Table of contents

Chapter 1: Introduction

1.1 Background

As the global economy grows and people increasingly rely on online offices, people are spending more and more time indoors. People spend an average of 80 to 90% of their time in indoor environments.[1][2]. Buildings are becoming more and more airtight, and when ventilation systems are not properly selected, indoor air quality will decrease and cause health problems, resulting in lower productivity. A comfortable and pleasant indoor thermal environment can enable indoor personnel to achieve a refreshing and good mental state and make people feel joyful.[3]

The primary purpose of ventilation is to provide acceptable indoor air quality and thermal comfort.[4] HVAC (Heating, ventilation, and air conditioning) system is the fastest and most effective way to meet human thermal comfort [3] by regulating air supply speed, indoor temperature, humidity and other relevant thermal environment parameters.

Since development of HVAC system, according to the direction of mechanical and thermal buoyancy, it can be divided into two main types: mixing ventilation (mechanical ventilation momentum and thermal buoyancy opposite) and displacement ventilation (mechanical ventilation momentum and thermal buoyancy the same).[5] As shown in Figure 1 and Figure 2.

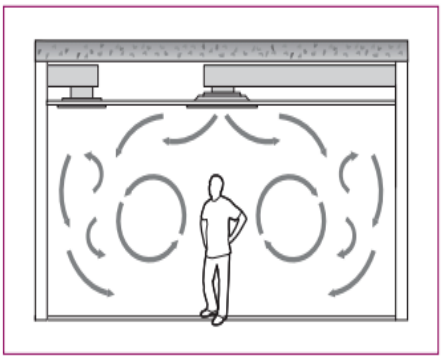

Figure 1 Mixing ventilation [6]

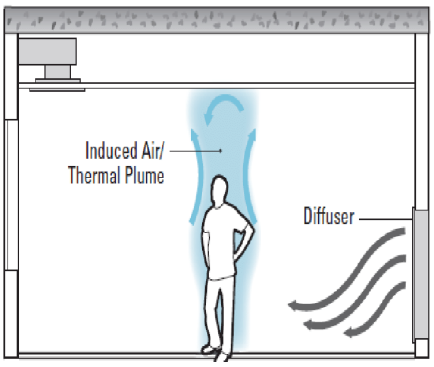

Figure 2 Displacement ventilation [6]

Displacement ventilation is difficult to use for winter heating, while energy consumption of mixing ventilation is too high, in order to overcome these problems, a new air distribution pattern known as air curtain jet (ACJ) ventilation [7] was presented. As shown in Figure 3.

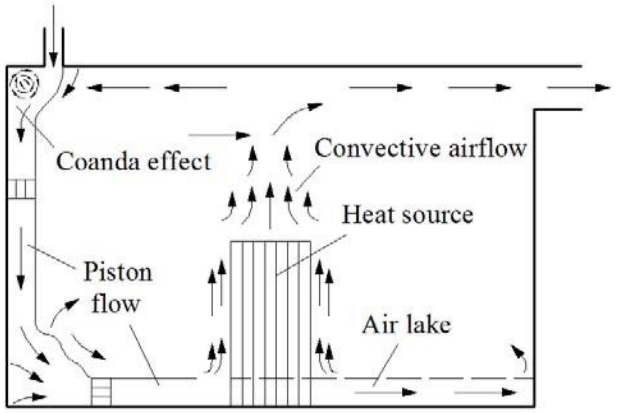

Figure 3 Air curtain jet ventilation [24]

At present, the most widely used ventilation methods are mixed ventilation and replacement ventilation, but the mixed ventilation method has high energy consumption and displacement ventilation cannot be applied to winter heating. Due to the disadvantages mentioned above, a new ventilation method combining the advantages of traditional ventilation system，known as air curtain jet (ACJ) ventilation [7] was proposed. Subsequently, a series of studies have been conducted on it, and all of them have shown that ACJ has good ventilation effects. However, the effect of this new ventilation method on high-intensity intensive heat sources has rarely been discussed.

1.2 Objectives

In this paper, a physical model of a room with 12 people sitting quietly in the office will be designed, where the people in the room and the electronic devices are used as heat sources to dissipate heat to the outside, in order to simulate a space with a dense distribution of heat sources and high heat load intensity. In addition, a working condition with reduced indoor personnel will be designed as a comparison, by reducing 12 people to 8 people to simulate the case of the reduction of heat load in the office

room.

Moreover, when considering that if there are more people in the room, the front row of people near the air conditioning supply vents are subjected to direct blowing, the wind speed is a big influence factor; besides, when considering whether the front row of people will produce a sense of cold, therefore the human thermal also needs to be discussed.

The research in this paper will be divided into two cases of high intensity heat source and low intensity heat source, adjust the air supply variables by changing the air supply speed (v=2m/s, v=1.5m/s), analyze the indoor flow field characteristics of using air curtain jet (ACJ) ventilation under different heat source conditions by CFD numerical simulation method and ANSYS Fluent software, plus calculate the thermal comfort, get the influencing factors of the vertical wall attached air supply method and the changes of airflow field when the heat source intensity changes. Finally, recommendations for the use of the new ventilation method will be made based on the conclusions of the analysis.

Chapter 2 Literature review

2.1 Traditional Ventilation

Since the development of the HVAC (Heating, ventilation, and air conditioning) system, the modes of ventilation can be divided into two main types: mixing ventilation ((mechanical ventilation momentum is opposite to thermal buoyancy) and displacement ventilation (mechanical ventilation momentum is the same as thermal buoyancy) [8] according to the direction of mechanical and thermal buoyancy.

2.1.1 Mixing ventilation

Mixing ventilation is the most widespread ventilation system.[9] The ventilation

system sends airflow into the room from the upper place of room at a relatively high speed, mixing it thoroughly with the room air and distributing it uniformly.[10]

When mixing ventilation is used in large spaces, the supply air jet is the first to pass through the upper non-working area, and then the return air is used to handle the work area load, which will result in energy waste. Meanwhile, the high momentum of the supply airflow, which also fully mixes the contaminants, which cause poor air quality.[11]

Although mixing ventilation occupies the mainstream form of the current ventilation and air conditioning market, it has lower ventilation efficiency and higher energy consumption compared with displacement ventilation.[12]

2.1.2 Displacement Ventilation

Displacement flow is defined as the movement of air within a space in a piston or plug-type motion.[13] Displacement ventilation sends airflow from the lower place of room at a lower speed, relying on the pressure difference due to the density difference as the driving force for the flow of air in the room. Since the supply airflow is cooler and sinks, the airflow flows downward, forming an airflow organization similar to an "air lake" at ground level. In upward flow process, the airflow continuously rolls up the surrounding airflow, and the thermal convection caused by the heat source makes the room produce a vertical temperature gradient: higher temperature at the top while lower temperature at the bottom.[14][15][16]

Displacement ventilation performs better comfort in living areas than mixing ventilation.[17] In addition, Awbi, H.B. [18] compared mixing ventilation and displacement ventilation systems by means of experimental methods and CFD numerical simulations, showing that displacement ventilation performs better ventilation efficiency and thermal comfort than mixing ventilation. [19]

However, because of the low air supply speed and small air supply temperature difference when using displacement ventilation, the indoor load is limited; in addition, the warm air flow tends to float under the action of floating force, so it is difficult to be

used for winter heating.[20]

2.2 Air curtain ventilation.

Displacement ventilation is difficult to use for winter heating, while the energy consumption of mixing ventilation is too high, in order to overcome these problems, air curtain jet (ACJ) ventilation [21] was presented. Air curtain jet ventilation is a new air distribution pattern, which has been developed by Coanda effect [22] and Impact Jet Ventilation (IJV).[23][24] It takes advantage of the wall-attached effect of the air supply jets and rationally controls the physical parameters of the jets to extend its range and maximize the expansion of the air supply along the floor. The airflow is transported to the working area, form a "lake of air" phenomenon and create an airflow organization similar to displacement ventilation.[25][26][27] As shown in Figure 4 and Figure 5.

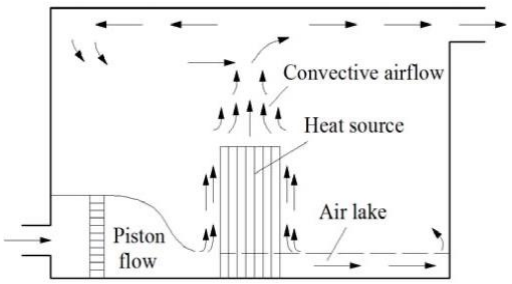

Figure 4. Explanation of displacement airflow.[24]

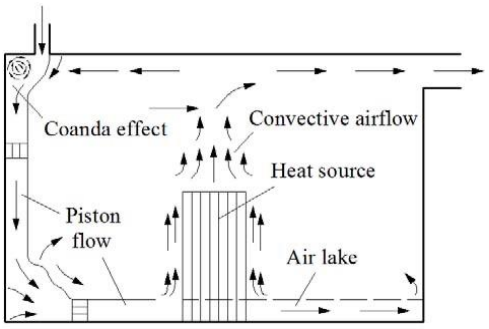

Figure 5. Explanation of air curtain ventilation. [24]

The Coanda Effect is the property of a jet of viscous fluid, when the fluid with a certain initial velocity from the orifice is shot out, will be rolled to absorb the surrounding environment fluid, the jet will be deflected toward the side of the fluid flow resistance, the jet is attracted to the nearby wall or with the convex wall on the wall to maintain contact.[28]

Due to the existence of a certain inertial momentum of the jet, will continue to maintain the original direction of flow along the surface, until the point of disengagement and the floor impact, the flow of air along the floor continues to remain attached to the floor flow phenomenon, known as the Extended Coanda Effect [29]，As

shown in Figure 6.

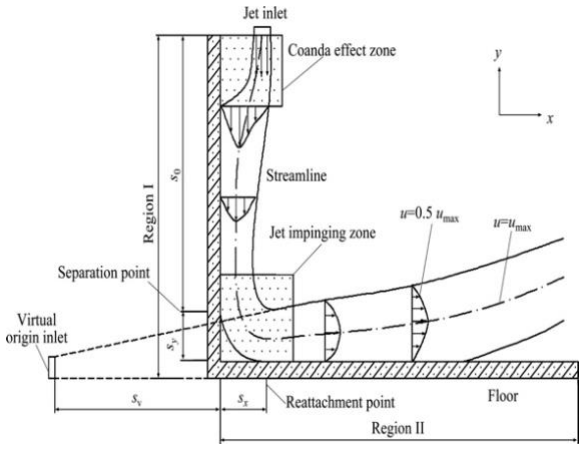

Figure 6. Coanda Effect [21]

H. Xue and C. Shu [30] used of two-dimensional turbulent flow model to calculate the velocity and temperature of the distribution of vertical wall attached jets under non-isothermal conditions. Crarft, T and Launder,B [31] used the pressure-stress model to study the flow law of three-dimensional turbulent advective jets, some unknown problems of three-dimensional turbulent flow attached jets were solved.

Y. Cho, H. Awbi [32] conducted theoretical studies and experiments of the multi-nozzle jets flow along vertical walls, compared them with displacement ventilation, which concluded that the "air lake" formed on the floor by the top-mounted multi-nozzle jet ventilation mode is better than the airflow organization effect of displacement ventilation.

Zhang, W [33] used visualization experiments to investigate the vertical wall-attached effect of adhesive jets and flow patterns in three regions: the horizontal air lake region, the vertical adhesion region and the impact deflection region. Established a more comprehensive qualitative understanding of the characteristics of the vertical wall-adhesive airflow organization.

Yin, H [34] proposed a design method for air curtain ventilation, and evaluated thermal comfort effectiveness of vertical wall-attached ventilation. The results showed

that the vertical wall attachment ventilation jet is a form of airflow organization with high ventilation efficiency and good thermal comfort for personnel in work area.

Wang, R [35] and He, X [36] showed that air curtain ventilation can provide good performance both in summer and winter.

2.3 Computational Fluid Dynamics (CFD)

When we study the fluid motion, the specific parameters in the flow field (such as density, velocity, temperature, pressure, etc.) with time and space, if we obtain empirical data through experimental methods, it not only takes time but also consumes a lot of human and material resources; in addition, for some practical engineering problems in tall spaces, it is difficult to do exactly the same laboratory simulation. If we start to analyze the air flow quantitatively from the theory, it is very difficult to solve it by analytical method. For these reasons, people gradually began to use computer technology to solve the problem of fluid flow, that is, computational fluid dynamics (CFD). [37]

The basic idea of CFD is that by discretizing the continuous physical field in space and time coordinates, control equations are transformed into a set of algebraic equations (i.e., discretization equation) on each node based on the discrete generation grid of the spatial and temporal domains of the computational model, and then solve the algebraic equations built up in this way to obtain an approximation of the requested variables. [38]

Finite difference method (FDM), finite element method (FEM), finite volume method (FVM) is commonly used methods for discretizing control equations, among them, FVM is currently the most widely used in the field of CFD. [39]

In 1987, CFD technology was first applied to HVAC (Heating, ventilation, and air conditioning) field, [40] since then, CFD simulation techniques have been widely used for the simulation of gas flow and airflow organization in ventilation spaces.

2.4 Thermal comfort

Thermal comfort is defined as the condition of mind which expresses satisfaction with the thermal environment. It is influenced by four indoor climate factors: air temperature, radiation temperature, air speed, humidity, clothing insulation and metabolic rate.[40]

Fanger P.O. created the thermal comfort evaluation index PMV-PPD model to describe the thermal feeling of human body.[41] Predicted Mean Vote (PMV) is defined as an index that predicts the mean value of the votes of a large group of persons, represents the perception of most people in the same environment.[40]

ASHRAE thermal sensation scale [40] is defined as follows:

thermal sensation	hot	warm	slightly warm	neutral	slightly cool	cool	cold
PMV	+3	+2	+1	0	–1	–2	–3

Table 1 the ASHRAE thermal sensation scale

and comfort standard is defined as -0. 5< PMV <0. 5, PPD<10%.[40]

However, PMV indicators may not represent the feelings of all individuals because of the physiological differences. Therefore, Fanger proposed the Predicted Percent Dissatisfied (PPD) index to represent dissatisfaction with the thermal environment. Predicted Percentage of Dissatisfied (PPD) is defined as an index that establishes a quantitative prediction of the percentage of thermally dissatisfied people determined from PMV. [40]

The relationship of PMV and PDD is as follows: [40]

$$\begin{aligned}\mathrm{PMV} &= [0.303\exp(-0.036\mathrm{M}) + 0.028] \times \mathrm{TL} \\ &= [0.303\exp(-0.036\mathrm{M}) + 0.0275] \\ &\times \{\mathrm{M} - \mathrm{W} - 3.05[5.73 - 0.007(\mathrm{M} - \mathrm{W}) - \mathrm{P_a}] \\ &- 0.0173\mathrm{M}(5.87 - \mathrm{P_a}) - 0.0014\mathrm{M}(34 - \mathrm{t_a}) - 0.42(\mathrm{M} - \mathrm{W} - 58) \\ &- 3.96 \times 10 - 8\mathrm{f_{cl}}[(\mathrm{t_{cl}} + 273)^4 - (\overline{\mathrm{t_r}} + 273)^4] - \mathrm{f_{cl}}\mathrm{h_c}(\mathrm{t_{cl}} - \mathrm{t_a})\}\end{aligned}$$

$$\mathrm{PPD} = 100 - 95\exp[0.03353\mathrm{PMV}^4 + 0.2179\mathrm{PMV}^2]$$

Where,

TL is the thermal load;

M is the metabolic rate, W/m^2;

W is the work rate, W/m^2;

P_a is the pressure of water vapor, kP_a;

t_a is the air temperature, °C ;

f_{cl} is the ratio of clothed /nude surface area;

t_{cl} is the clothing surface temperature, °C;

h_c is the convective transfer coefficient, $W/(m^2 \cdot K)$;

$\overline{t_r}$ is the Mean Radiant Temperature, °C.

Chapter 3 Materials and methods

3.1 Geometry

The physical model was designed as an office with dimensions of (L × W × H) 6.5mx5.5mx3m. A slit air conditioner inlet and air conditioning return outlet and 2 fluorescent lights are installed on the ceiling. 2 desks are located in the middle of the room, 12 laptops are placed on the desks and 12 people sit in silence. At the back of the room, a table and a printer are placed. The layout is shown in Figure 7.

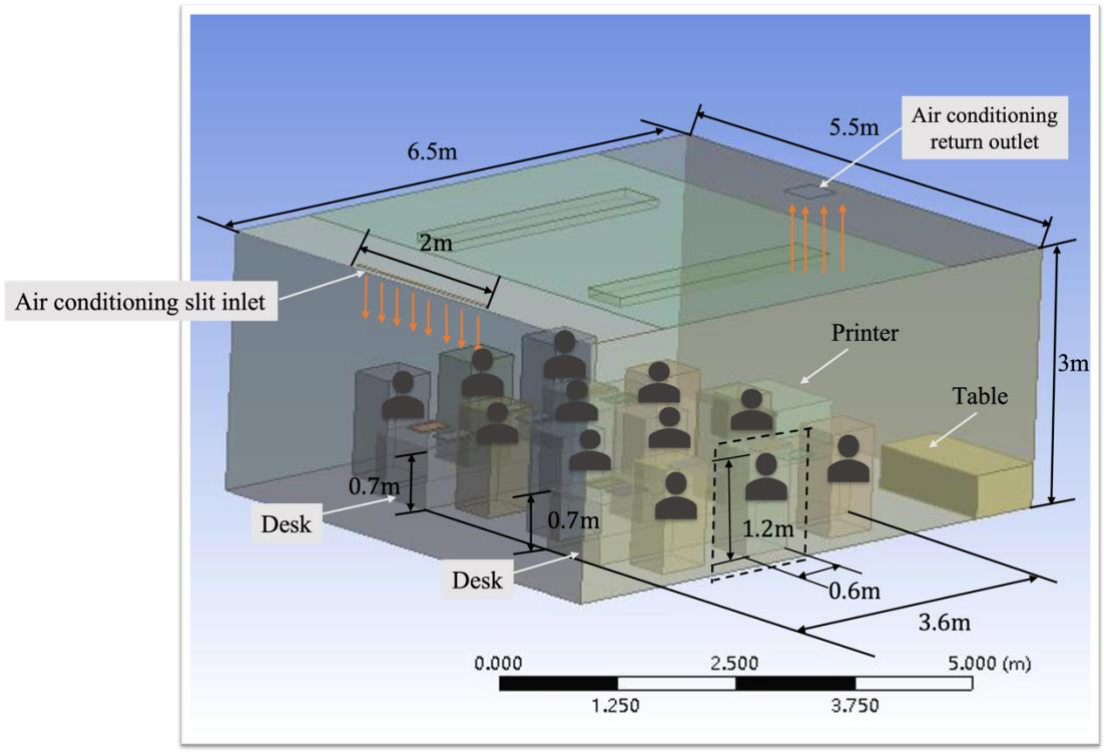

Figure 7. Layout of the room

The dimensions of the other objects are shown in Table 2.

people	$0.6\text{m} \times 0.5\text{m} \times 1.2\text{m}$（L × W × H）
desk	$3.6\text{m} \times 0.8\text{m} \times 0.7\text{m}$（L × W × H）
laptop	$0.4\text{m} \times 0.22\text{m} \times 0.02\text{m}$（L × W × H）
table	$1.5\text{m} \times 0.8\text{m} \times 0.5\text{m}$（L × W × H）
printer	$1\text{m} \times 0.8\text{m} \times 0.5\text{m}$ (L × W × H)
lamp	$3\text{m} \times 0.5\text{m}$ (L × W)
inlet	$2\text{m} \times 0.05\text{m}$ (L × W) $s = 0.1\text{m}$（s is the vertical distance between the air vent and the wall）
outlet	$0.4\text{m} \times 0.4\text{m}$ (L × W)

Table 2. Dimensions of the other objects

3.2 Turbulence models

3.2.1 Governing equations

The general fluid flow is controlled by basic control equations which determine the fluid motion. There are three major conservation laws of physics: Mass Conservation Equation, Energy Conservation Equation and Momentum Conservation Equation. Viscous fluid motion model can be described by the three-dimensional Navier-Stokes equation (N-S equation) and solved by Reynolds averaging method. Reynolds-averaged Navier–Stokes equations (RANS) [42] method assumes that the flow field variables in the N-S equation consist of two components, the instantaneous mean and the pulsation. By introducing turbulent momentum, heat and mass diffusion coefficients through the Boussinesq assumption, relate the turbulent pulsation values to the time-averaged values, the turbulence calculation is transferred to ratio coefficient calculation between Reynolds-stress and strain (i.e., turbulent viscosity coefficient). Which reduce the computational loads and save space and time. It is the reason that the RANS method has become the most widely used method for numerical simulation of turbulence.

The Governing equations based on the Reynolds averaging method (RANS)

include [42] :

Mass Conservation Equation

$$\frac{\partial \rho}{\partial t}+\frac{\partial(\rho \overline{u}_i)}{\partial xi}=0$$

Momentum Conservation Equation

$$\frac{\partial(\rho \overline{u}_i)}{\partial t}+\frac{\partial}{\partial x_j}(\rho \overline{u}_i \overline{u}_j)-\frac{\partial}{\partial x_j}\left[\mu\left(\frac{\partial \overline{u}_i}{\partial x_j}+\frac{\partial \overline{u}_j}{\partial x_i}\right)-\rho \overline{u_i' u_j'}\right]=-\frac{\partial \overline{p}}{\partial x_i}+S_i$$

Energy Conservation Equation

$$\frac{\partial(\rho T)}{\partial t}+\frac{\partial\left(\rho u_j T\right)}{\partial x_j}=\frac{\partial}{\partial x_j}\left(\frac{\lambda}{c_p}\frac{\partial T}{\partial x_j}-\rho \overline{u_j' T'}\right)+S_T$$

Where,

u_i is the fluid velocity;

p is the pressure;

ρ is the density;

μ is the fluid kinematic viscosity;

t is the time;

T is the temperature;

S is the Source item.

3.2.2 Selection of turbulence equations

Reynolds stresses ($\rho \overline{u_i' u_j'}$) occurs after Reynolds averaging of the momentum equation, and the RANS equations for each stress component of the convective transport equation need to be solved. If the Reynolds averaging of the stress components of the convective transport equation continues, it will lead to the appearance of higher order unknowns（$\overline{u_i' u_j' u_k'}$）, this will lead to an infinite number

of unknowns, and the whole set of equations will never be closed. In this way, it is necessary to use some specific relations that relate the additional term of the turbulent pulsation values to the time-averaged values (i.e., the turbulence model) to close the set of equations.

Depending on the assumptions made or the treatment of the Reynolds stress term, there are two main categories of RANS turbulence models: Reynolds stress models and vortex viscosity models. Among them, Reynolds stress models include algebraic stress models and Reynolds stress transport equation models, [43] in which differential equations are directly developed and solved for turbulent pulsating stresses. This type of method is usually computationally intensive and requires high computer requirements. Vortex viscosity models, including zero-equation models, one-equation models, and two-equation models (e.g., k - ε models, k - ω models). [44]

K-ω model is one of the most commonly used turbulence models, [46] it is more applicable to uniform counterpressure flow and better predict the performance of strong streamline bending and corner flow. The SST k-ω model is a modified form of the standard k-ω model, it has same predictive properties of the k-ω model in the near-wall region and far-wall region. In addition, SST k-ω model can successfully simulate the associated thermal stratification phenomena and thermal plume structure. [46]

Yin, H and Li, A [45] used computational fluid dynamics methods to compare the four turbulence models: standard k-ε, SST k-ω, RNG k-ε and RSM-IP model. They also conducted a full-scale experiment. SST k–ω model produced the best result.

3.3 Discretization

The Meshing component of ANSYS Fluent 2021 R2 software is used for discretization. Finite Volume Method (FVM) discretizes the physical model by structured hexahedral structure.

3.3.1 Grid independence validation

The grid division influences the precision of the calculation results and also

affects the calculation efficiency. Therefore, both computational accuracy and computational efficiency should be considered when selecting the number of grids. The calculation results of velocity and temperature when 11 points are randomly selected to check different grid numbers are shown in Fig.8 and Fig.9. The results show that both velocity and temperature do not differ much. The difference of velocity is not more than 0.1 m/s, the difference of temperature is not more than 3 ℃. Considering the calculation time, the number of grids is chosen as 137502.

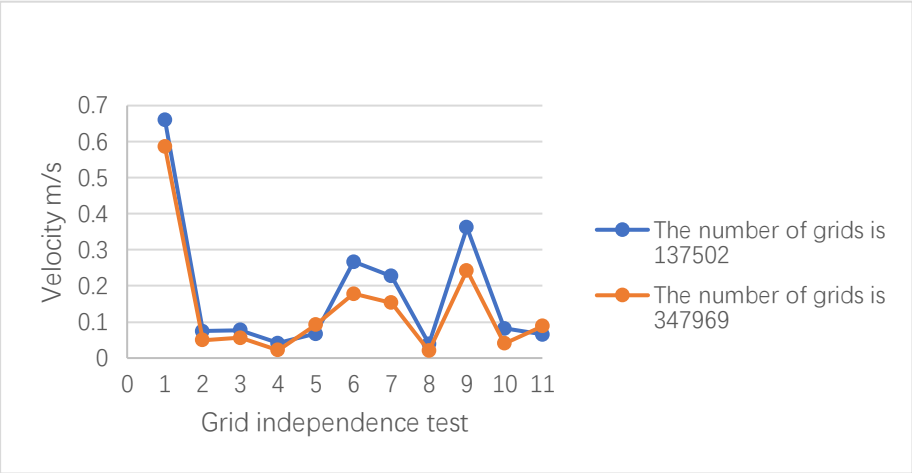

Figure 8

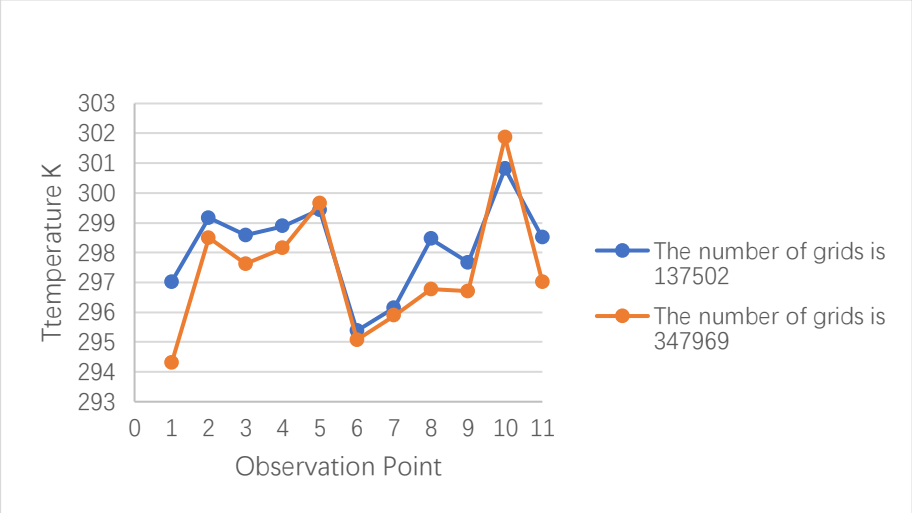

Figure 9

3.3.2 Grid division

Cross-sectional in the xy-plane, z = 1.5 m.

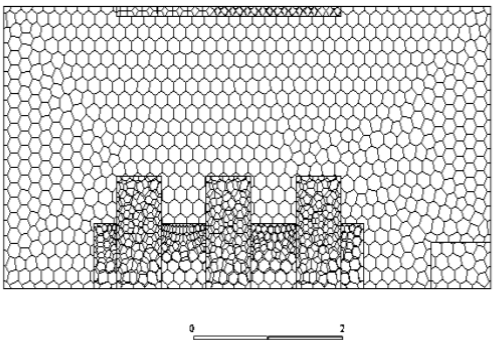

Figure 10

After the mesh independence verification, the number of meshes is determined as 137502, is shown in Fig10.

3.4 Numerical simulation

3.4.1 Boundary conditions

To simplify the problem, the following assumptions are made about the indoor flow field:

The air in the room is a steady-state, incompressible fluid that conforms to the Boussinesq assumptions.

Ignore the heat radiation between the solid walls.

The airtightness of the doors and windows in the room is good, and there is no air leakage effect.

Isobaric flow in accordance with the equation of state of the gas.

Air in the room is incompressible three-dimensional unsteady turbulence, the air can be considered as an ideal gas, the variation of density with temperature is in accordance with Boussinesq hypothesis, and the solid walls are all stationary without sliding walls. The boundary conditions are set as shown in Table 3.

Item	Boundary condition	
person	heat flux	$25\mathrm{W}/\mathrm{m}^2$
laptop	heat flux	$15\mathrm{W}/\mathrm{m}^2$
printer	heat flux	$34\mathrm{W}/\mathrm{m}^2$
lamp	heat flux	$34\mathrm{W}/\mathrm{m}^2$
table	heat flux	$0\mathrm{W}/\mathrm{m}^2$ (Adiabatic boundary)
desk	heat flux	$0\mathrm{W}/\mathrm{m}^2$ (Adiabatic boundary)
wall, floor, roof	heat flux	$0\,\mathrm{W}/\mathrm{m}^2$ (Adiabatic boundary)
outlet	outflow	
inlet	velocity-inlet	V_1=2m/s, V_2=1.5m/s, T=293.15K, D_H=0.09m, I=5%

Table 3. Boundary conditions

Where

V is the Velocity Magnitude [m/s]

T is the Temperature [K]

I is the Turbulent Intensity [%]

D_H is the Hydraulic Diameter [m]

3.4.2 Solver Settings

In this study, air fluid is considered as a three-dimensional continuous incompressible fluid, flow are constant.

Since the simulation involves temperature, it is also necessary to start the energy equation and to consider the effect of gravity by setting the gravitational acceleration along the vertical direction. The Pressure Based Implicit format is chosen, the Second Order Upwind format is used for the discrete format of the convection term, and the Pressure-Velocity Coupling method is used for the SIMPLE algorithm.

The calculation uses a non-stationary solution with a time step size of 3 s per iteration, 20 max iterations per step, and 600 iteration time steps. In another way, the room is considered to reach a steady state temperature in 30 minutes (i.e.,1800 s).

3.4.3 Model convergence determination

From Table 4, it is seen that the model calculation results converge

	Value	Absolute Criteria	Convergence Status
continuity	6.956113e-06	0.001	Converged
x-velocity	4.929147e-05	0.001	Converged
y-velocity	6.028996e-05	0.001	Converged
z-velocity	0.0001452449	0.001	Converged
energy	3.313124e-07	1e-06	Converged
k	5.79756e-05	0.001	Converge
omega	4.72907e-05	0.001	Converged

Table 4

3.4.4 Validation of the results

This section compares the numerical simulation results with the literature studies to verify the accuracy.

Results are as follows：

(1) Comparison of the numerical simulation results with the experimental results in the literature [35] (Figure 11):

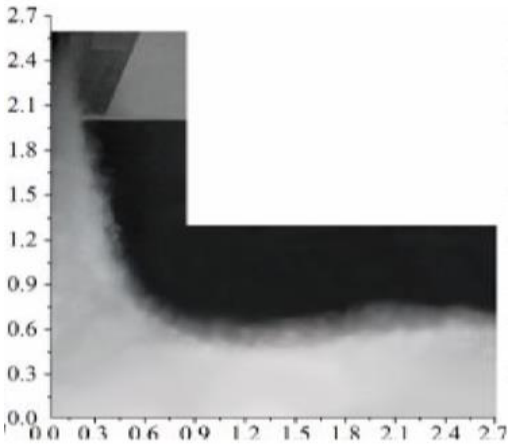

Figure 11

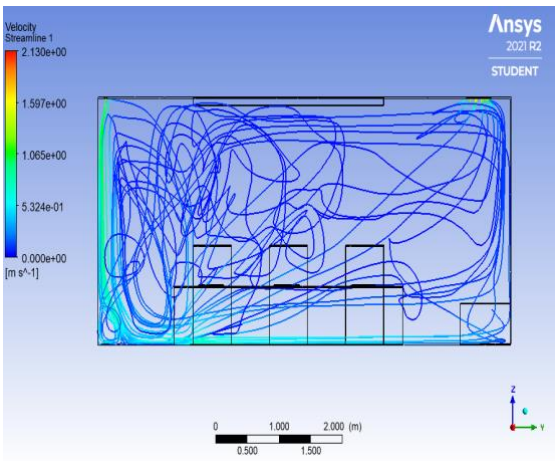

Figure 12

(2) Comparison of the numerical simulation results with the theoretical diagram in the literature [21] (Figure 13):

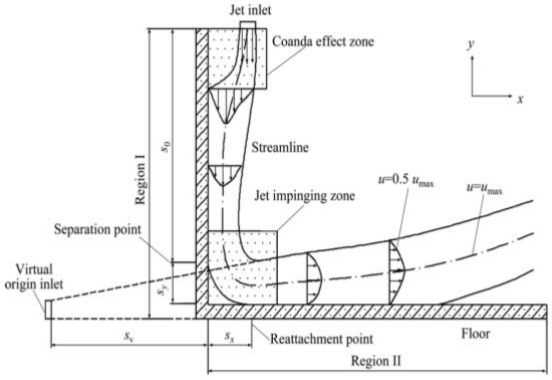

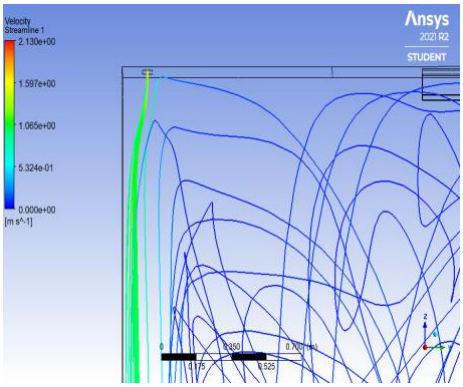

Figure 13 Figure 14

The Coanda effect phenomenon was successfully simulated using the SST k-ω model. As can be seen from the traces of the numerical simulation results (Figure 12,14), the airflow adheres to the wall and spreads against the ground, successfully forming an "air lake".

Chapter 4: Simulation results and analyzation

4.1 The effect of air supply speed on the overall velocity flow field

4.1.1 Results Analysis

Case 1: X=2.7m

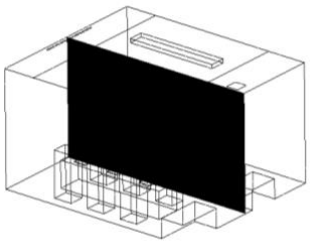

Velocity Contour

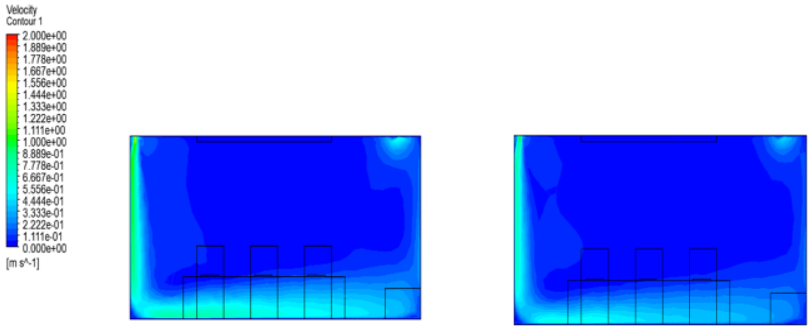

$v = 2m/s$ $v = 1.5m/s$

Figure 15

From the velocity distribution diagram (Figure 15) of case 1 (cross-section at the center of the air outlet), it can be seen that the airflow is sent straight down from the slit air outlet at the top of the room, attached to the vertical wall to support vertical downward flow and sinks by gravity. Due to the existence of the inverse pressure gradient, the jet flows along the vertical wall until it impacts with the floor and changes direction, turning to the horizontal direction and spreading along the floor to form a layer of air lake near the floor.

From the case 1, it can be intuitively seen, because there is no object to obstruct

the flow of gas, the wind speed from the air supply outlet to the ground basically unchanged, the airflow in the horizontal direction after a certain distance attached to the wind speed decreases in a gradient. At the wall near the air supply outlet, the airflow velocity at the ground attachment area and the return air outlet is the largest, which is maintained in the range of 1.2m/s～0.5m/s.

The wind speed in the lower half of the air lake in the vertical direction is significantly greater than the upper half of the region, and the vertical speed gradient mainly exists at about 0.5m to 0.7m. The airflow speed in the above region is stable and basically in the speed range of 0m/s～0.3m/s. The air supply airflow above the working area is less mixed with the surrounding ambient air and remains stationary without being disturbed by the air supply airflow. When the wind speed is reduced from 2m/s to 1.5m/s, the airflow organization and velocity field distribution of the characteristic section at the air supply outlet is basically the same. The difference in wind velocity distribution pattern is not much, but the overall wind velocity is slightly different.

Case 2: X=3.05m

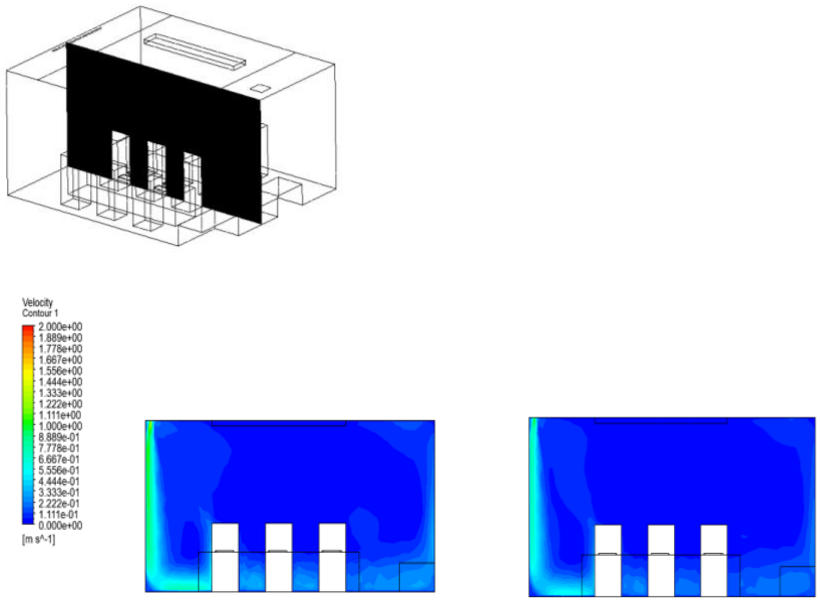

$v = 2m/s$ $v = 1.5m/s$

Figure 16

It can be seen from Figure 16 that the airflow is basically the same as that in Case 1, the airflow is sent straight down from the slit air outlet at the top of the room, attached to the vertical wall to support the vertical downward flow, and sinks by the action of gravity. Due to the existence of the inverse pressure gradient, the jet flows along the vertical wall until it impacts with the floor and changes direction, turning to the horizontal direction and spreading along the floor to form a layer of air lake near the floor. Due to the obstruction of indoor equipment, the wind speed in the back half of the work area is reduced, creating a weaker lake of air above the floor.

The air supply airflow above the working area is less mixed with the surrounding ambient air and is basically not disturbed by the air supply airflow.

Case 3: X=1.95m

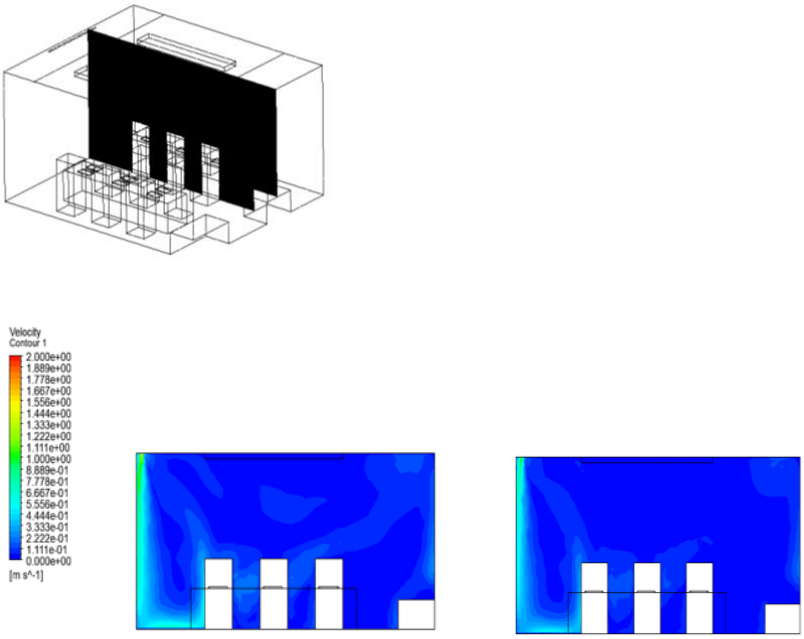

$v = 2m/s$ $v = 1.5m/s$

Figure 17

It can be seen that the airflow is sent straight down from the slit air outlet at the top of the room and attached to the vertical wall; Because of t the presence of the inverse pressure gradient, the jet flows along the vertical wall until it impacts with the floor and changes direction, turning horizontal and spreading along the floor. The airflow should

have spread in the horizontal direction against the ground to a certain distance, but because the air encounters the indoor obstructions, the wind speed changes drastically, and the airflow escapes everywhere. Therefore, the wind speed in the latter half of the working area is very small, and there is basically no air lake phenomenon. The maximum wind speed is at the edge of the wall and the front wall, which is kept in the range of 0.5m/s to 1m/s. When the wind speed is 2m/s, backflow is generated above the working area, and the air is spinning above; the velocity distribution shows cyan surrounded by blue, which is an obvious vortex phenomenon. After the formation of vortex, after a period of air supply, so that the local wind speed increased by 0.1m/s, the velocity field distribution is not uniform, when the air supply speed is reduced to 1.5m/s, the overall indoor wind speed changes also become smaller, the maximum wind speed of the work area where the personnel is 0.2m/s.

Case 4: X=1.5m

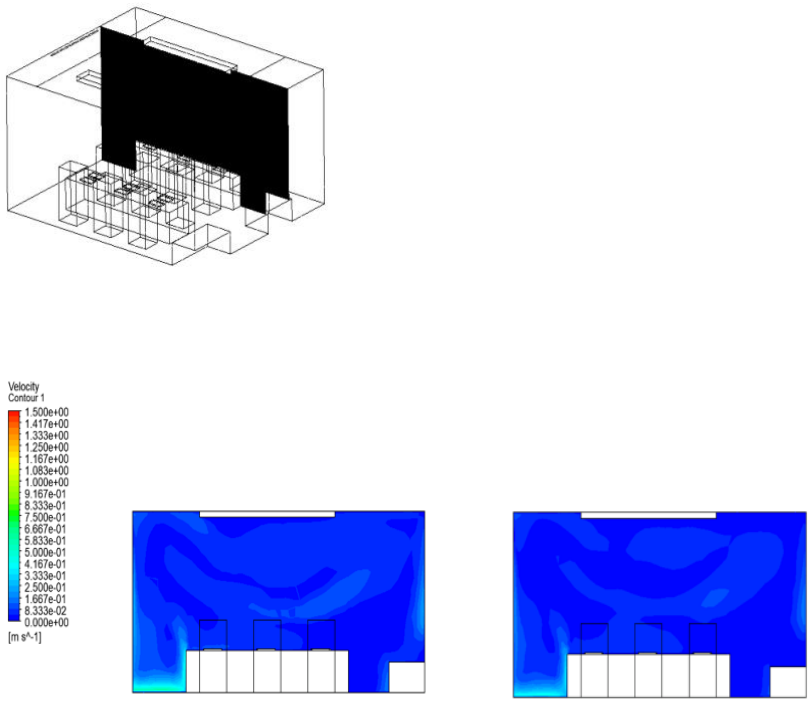

$v = 2m/s$ $v = 1.5m/s$

Figure 18

As can be seen in Figure 18, the maximum wind speed appears at the ground level

on the left side of the figure with a wind speed of 0.4 m/s. After the airflow adheres to the floor at a certain distance in the horizontal direction, the inertial force is weakened, the horizontal adherence range is limited, and the airflow is blocked by the desk, the airflow direction is changed and a vortex structure with an obvious wind speed gradient is formed, the wind speed difference is about 0.1 m/s. The indoor flow field is more turbulent in the height direction.

Case 5：X=0.35m

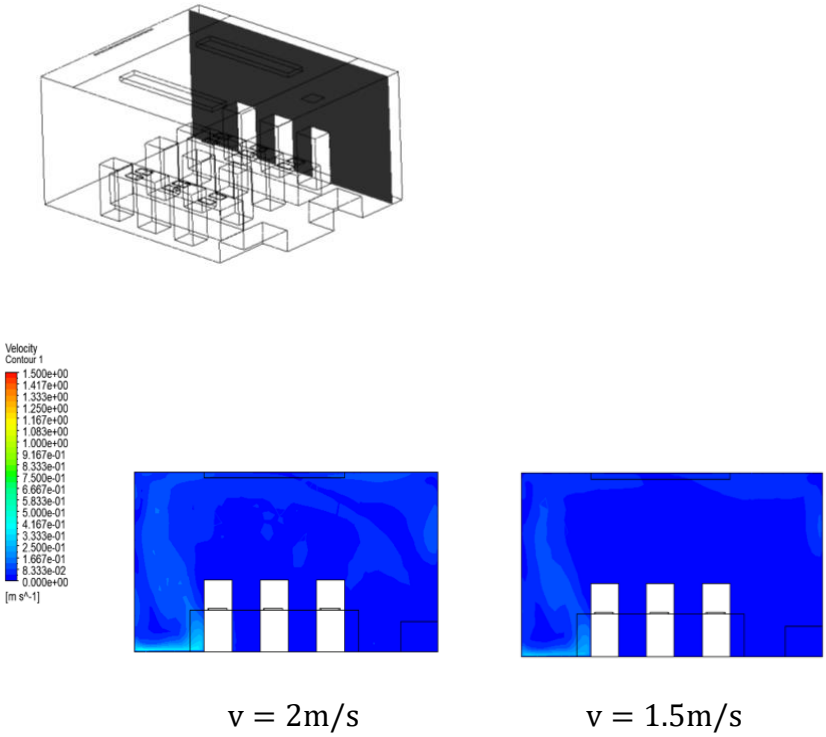

$v = 2m/s$ $v = 1.5m/s$

Figure 19

As this section is far from the air outlet, the maximum wind speed is basically located at the ground level in the front of the room corresponding to the air outlet, and the maximum wind speed is only 0.4 m/s. This is due to the airflow in the horizontal direction after a certain distance of attachment, the inertial force is weakened, and the horizontal attachment range is limited, so the air conditioning air cannot reach the result.

4.1.2 Summary

Using the new wall-mounted ventilation method, the airflow is sent straight down from the slit air outlet at the top of the room at different air supply speeds and flows vertically downward by attaching to the vertical wall, separating from the vertical wall at about 0.5 m in the vertical direction and changing direction. The air flow is diverted to diffuse forward along the horizontal floor and forms an air lake on the floor.

With the characteristic cross-section gradually moving away from the air outlet (cases 1 to 5), the large wind speed area is mainly concentrated on the floor and the wall near the side of the air outlet. In addition, the airflow in the horizontal direction after a certain distance, the inertial force is weakened, the horizontal attachment range is limited, the air cannot reach the location far away from the air conditioning outlet too far, the cool air does not completely affect the entire room area, so the room tends to show an imbalance between hot and cold. As the cross-section gets closer to the air outlet, the distribution of the air velocity field becomes more regular, and the wind speed is gradually smoothed.

When there are no objects to block (such as case 1), an ideal air lake-like velocity distribution can be formed in the working area. When the ground air supply intersects with indoor equipment and personnel (such as case 2 to 5), the free flow of gas is obstructed, disrupting the route of the fluid and generating vortex phenomenon, and the wind speed changes sharply at the intersection. When the air volume is not large enough, the air will escape in all directions.

4.2 The effect of air supply speed on the overall temperature flow field

4.2.1 Results Analysis

Case 1.1: X=2.7m

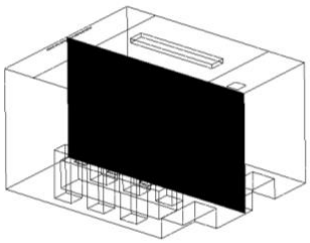

Temperature Contour

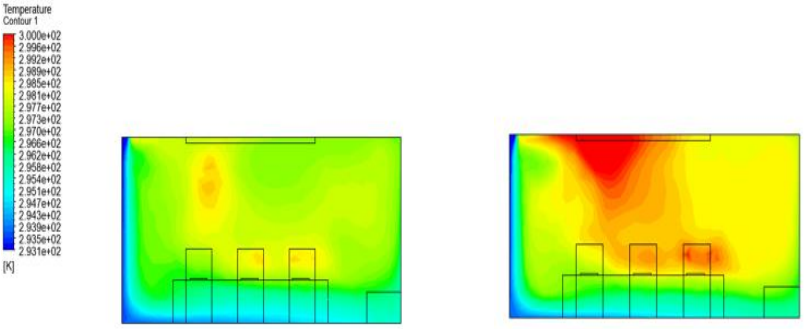

$v = 2m/s$ $v = 1.5m/s$

Figure 20

Since the vertical wall is attached to the air supply, the temperature gradient spreads to the room from the air supply outlet and has a large impact on the temperature of the surrounding area.

From the temperature contour, when the air supply speed of the air conditioner is 2m/s, it can be seen that the overall temperature distribution is more uniform. The maximum temperature difference in the working area where personnel are concentrated is 2℃, and the maximum temperature is 25℃. When the wind speed is reduced to 1.5m/s, a high temperature group appears in the area where personnel are concentrated,

and the maximum temperature reaches 26℃ and the temperature field is obviously stratified, the space appears to have inconsistent temperatures.

Case2.1: X=3.05m

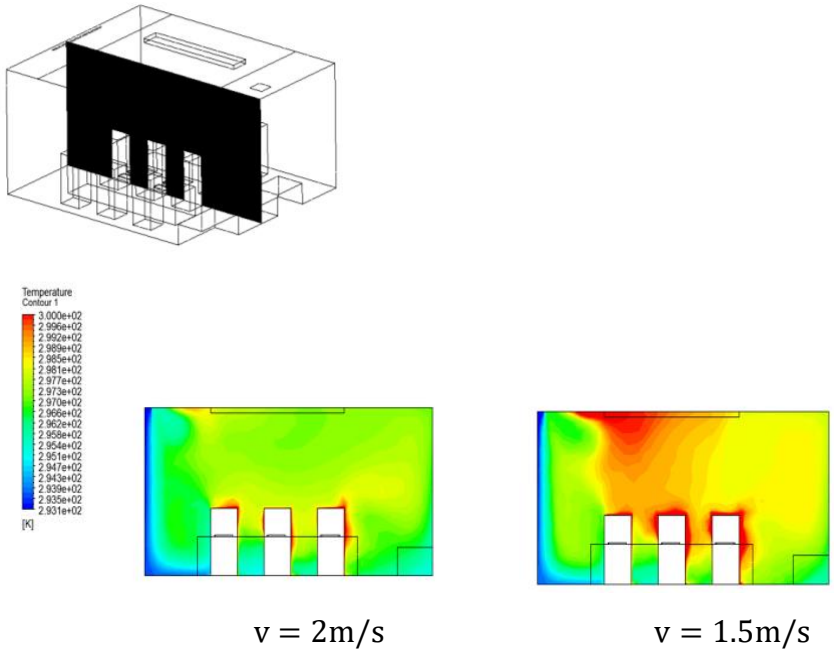

$v = 2m/s$ $v = 1.5m/s$

Figure 21

When the wind speed is large enough, that is, v=2m/s, under the action of the air lake, from the cross-section, the cooling effect is better, the temperature gradient is more uniform, when the wind speed is reduced to 1.5m/s, the cold air does not have enough power to discharge the indoor heat load, so there is thermal aggregation above the work area area, there are multiple temperature gradients, the distribution of the temperature field is chaotic.

The highest temperatures were all found in the vicinity of the human body, due to the fact that the human body is considered as a heat source in this study and radiates heat outward.

Case 3.1: x=1.95m

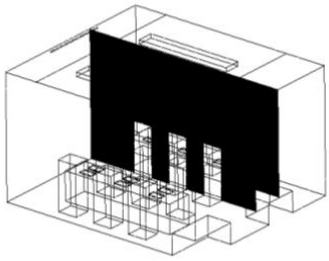

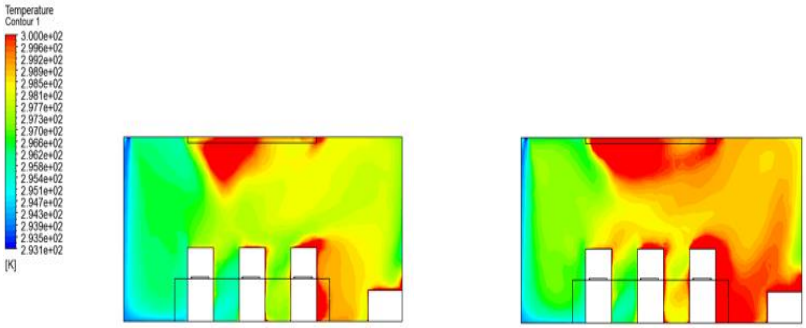

$v = 2m/s$ $v = 1.5m/$

Figure 22

Case 4.1: X=1.5m

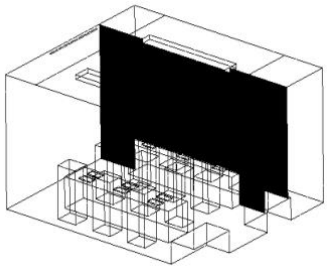

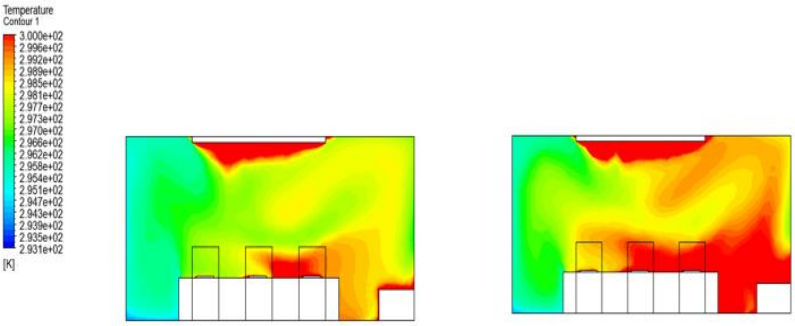

$v = 2m/s$ $v = 1.5m/s$

Figure 23

As can be seen in case 3.1 and case 4.1, As the characteristic cross-section

gradually moves away from the air conditioning supply, high temperature clusters appeared on the right side of the graph (i.e., at the back end of the room) and at the roof, reaching a maximum temperature of 27℃.

In the working area near the back half of the room, heat is dissipated to the outside due to the existence of heat sources, moreover, the heat source obstructs the diffusion of the airflow, air flows back between the equipment and the walls, causing the temperature of the supply airflow to increase as well, resulting in poor cooling effect. Vortex phenomenon occurs in this area, so the temperature field distribution on the right side becomes complicated. Even when use the larger air supply velocity (v=2m/s), multiple significant temperature gradients appear, and the temperature field is very non-uniform.

Case 5.1: X=0.35m

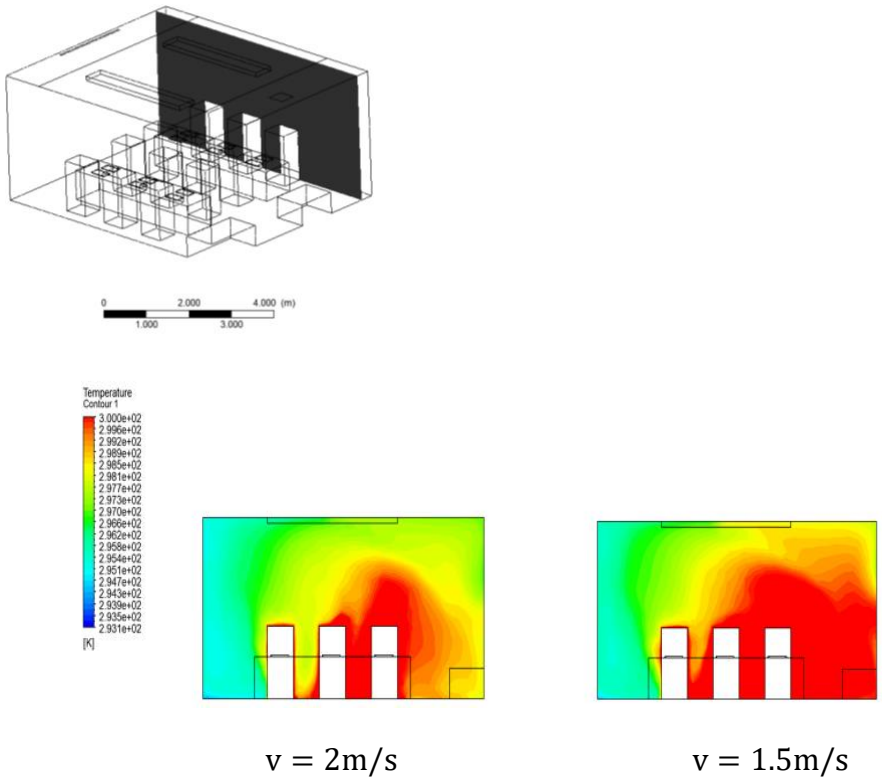

$v = 2m/s$ $v = 1.5m/s$

Figure 24

From the figure, the overall temperature field shows a clear temperature gradient, when air supply speed decreases, a high-temperature aggregation with a clumped distribution shows on the right side of the cloud map (i.e., the back end of the room).

4.2.2 Summary

The distribution of the temperature field is related to the air speed of the air conditioning. When the characteristic section is close to the air conditioning equipment outlet, temperature field distribution of the section become uniform. Due to the Coanda effect, where the airflow is attached to the walls.

The smaller the inertial force of the air flow adhering to the ground to deliver air, which impedes the spread of cold air. The cool air cannot have an impact on the room as a whole, and it is difficult for the airflow to be adequately delivered to the working area.

In case 1.1 and case 1.2, the main body of air supply flows through the area, and it can be seen that the temperature field of the room is distributed more evenly, excluding the existence of obvious temperature gradient near the wall and floor, and the overall temperature gradient is small. Generally, when the speed is reduced from 2m/s to 1.5m/s, the temperature field distribution on the characteristic cross-section becomes chaotic and disorderly, with high temperature gathering in many places. Therefore, when there are more people in the room and the heat load is large, a larger wind speed should be selected.

4.3 Existing problems

After the airflow blows out from the air supply outlet, when it intersects with the obstacle, the trajectory of airflow changed. Airflow is difficult to spread to a greater distance. The distribution of indoor airflow organization is not uniform, and it is difficult to send air to all corners of the room. Vortex phenomenon is easy to be produced in the distribution of temperature and velocity fields.

Due to the obstruction of indoor personnel and objects, the airflow is hindered and cannot be quickly diffused to all parts of the room (especially the back half of the room), office workers in the room will feel stuffy and unbearable hot, cannot achieve the cooling effect.

Chapter 5. Comparative study under reduced heat source conditions

Based on the analysis in the previous chapter, it is concluded that the indoor heat load and the degree of diffusion of the floor-adhering jet have a very important effect on the indoor cooling effect and airflow distribution. Therefore, in this chapter, the number of indoor personnel is reduced in order to decrease the intensity of the heat source, and the flow field variation will be discussed for the same boundary conditions and air supply conditions.

5.1 Geometry

The physical model was designed as an office with dimensions of (L × W × H) 6.5mx5.5mx3m. In this office, a slit air conditioner is installed in the ceiling at the front of the room. 2 desks are located in the middle of the room, and 12 laptops are placed on the desks, where 8 people sit in silence. At the back of the room, a table and a printer are placed. In addition, there are 2 fluorescent lights and air conditioning return vents on the ceiling. The layout is shown in Figure 25.

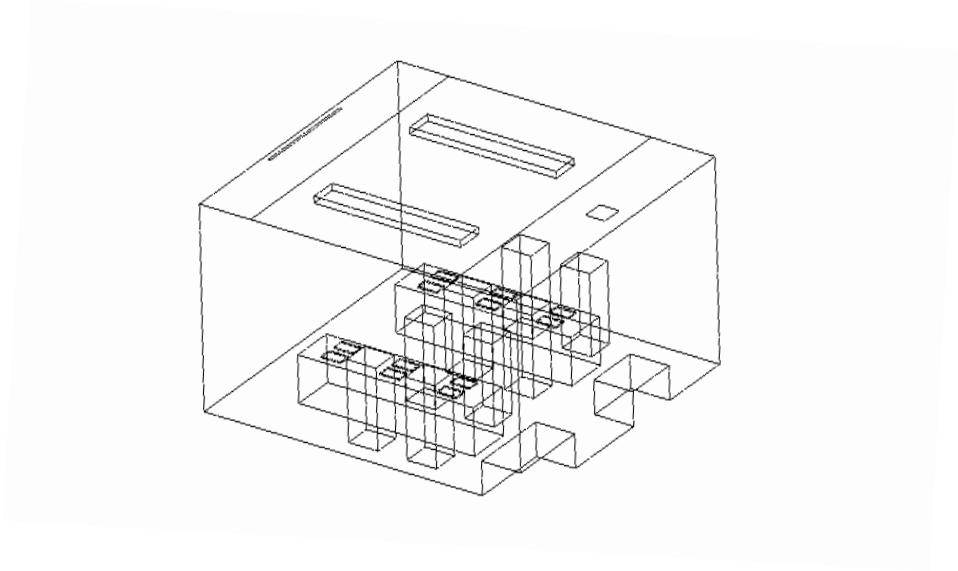

Figure 25

5.2 Comparison results

$x = 2.7m$ Velocity contour Temperature contour

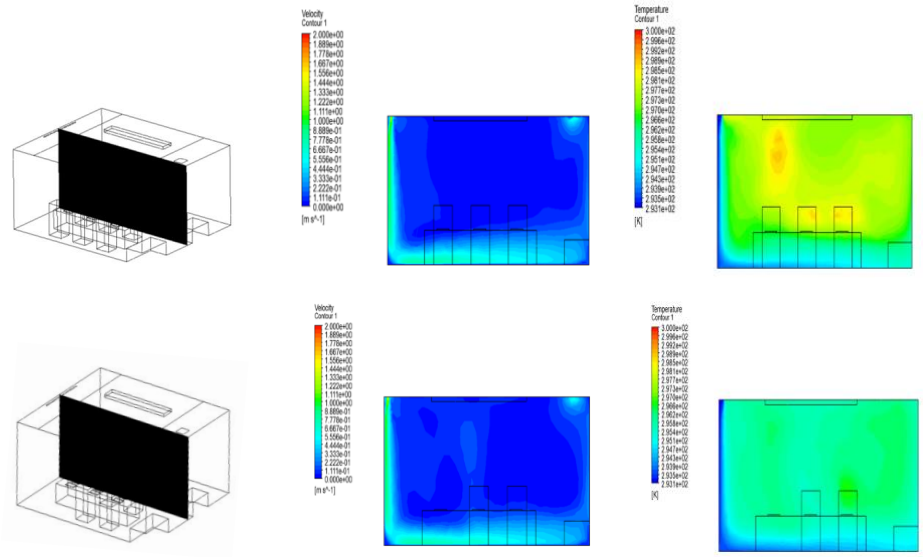

Figure 26

$x = 3.05m$

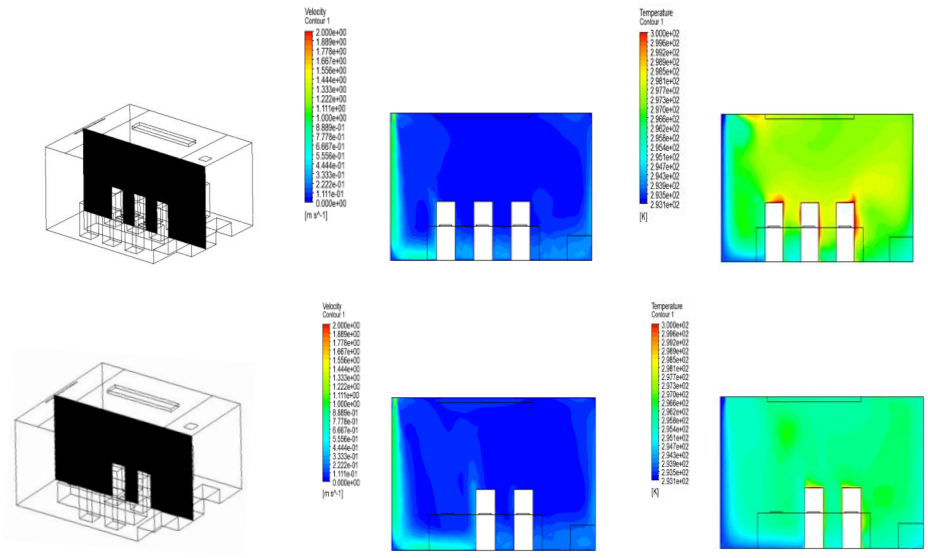

Figure 27

$x = 1.95m$

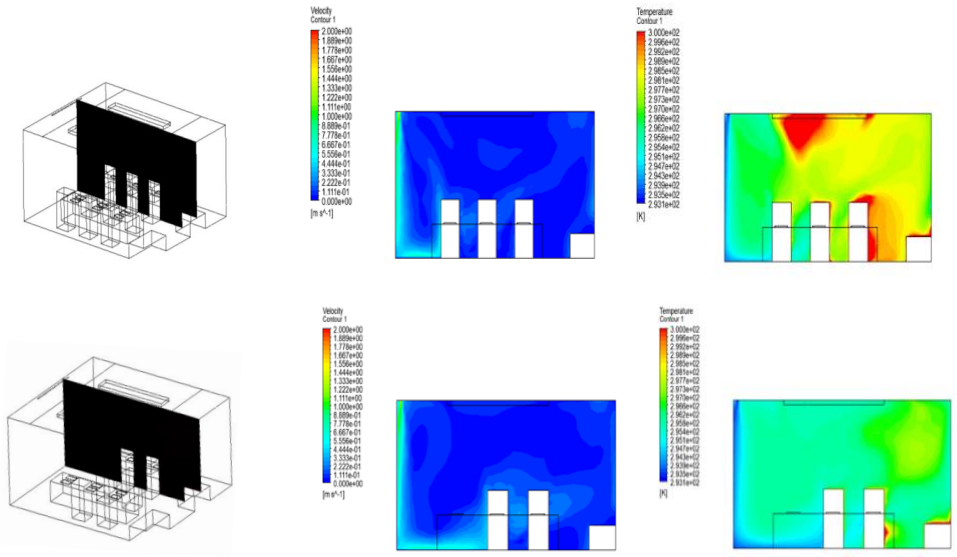

Figure 28

$x = 1.5m$

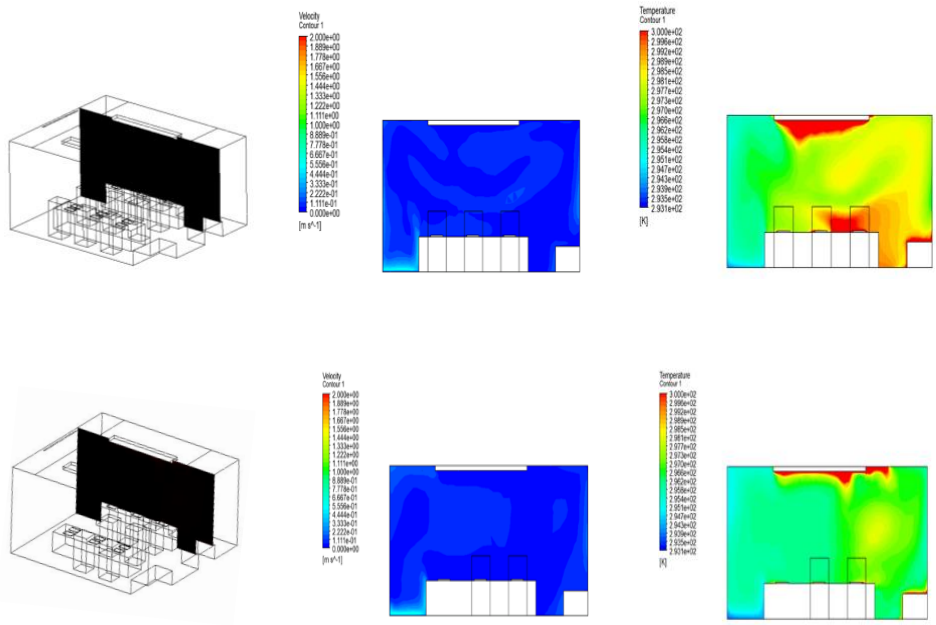

Figure 29

$x = 0.35m$

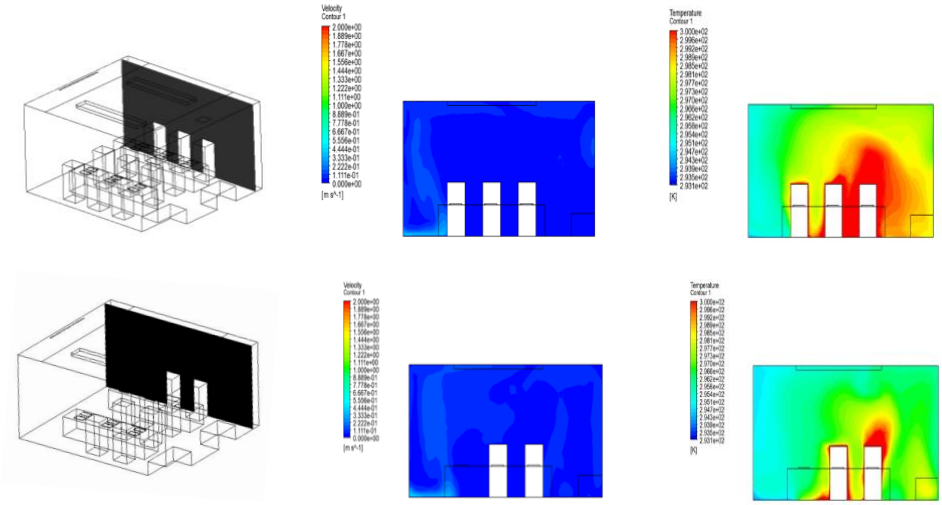

Figure 30

After reducing the personnel, air supply is mixed with the room air more adequately, the temperature field becomes uniform, and the fluctuation of each section is moderated. It shows that the range of cold air can affect this room has increased.

5.3 The effect of air supply speed on the overall speed and temperature flow field

$Case\ 1.2\ x = 2.7m$

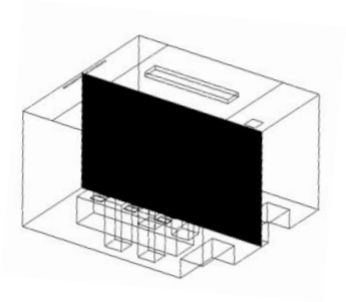

Velocity Contour

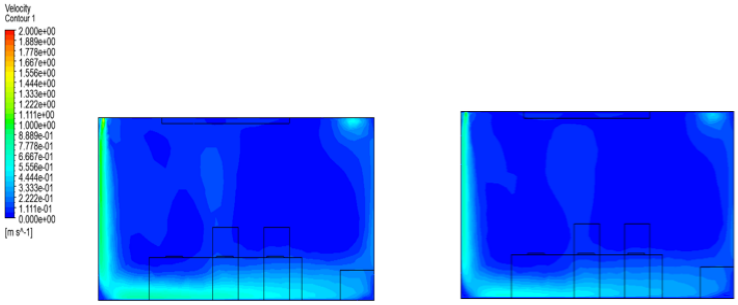

$v = 2m/s$ $v = 1.5m/s$

Temperature Contour

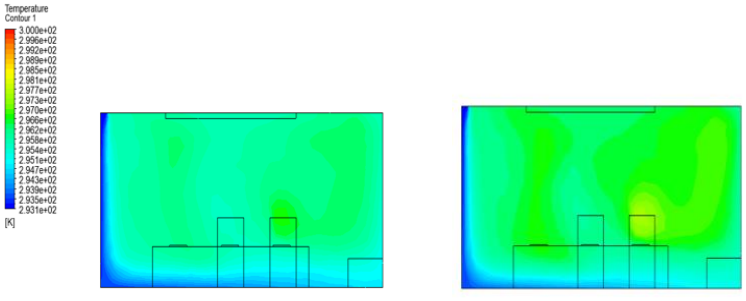

$v = 2m/s$ $v = 1.5m/s$

Figure 31

$Case\ 2.2\ x = 3.05m$

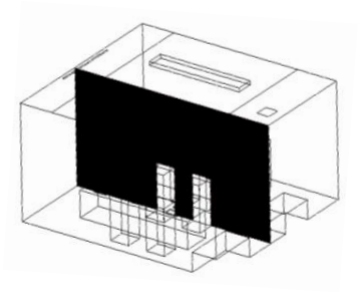

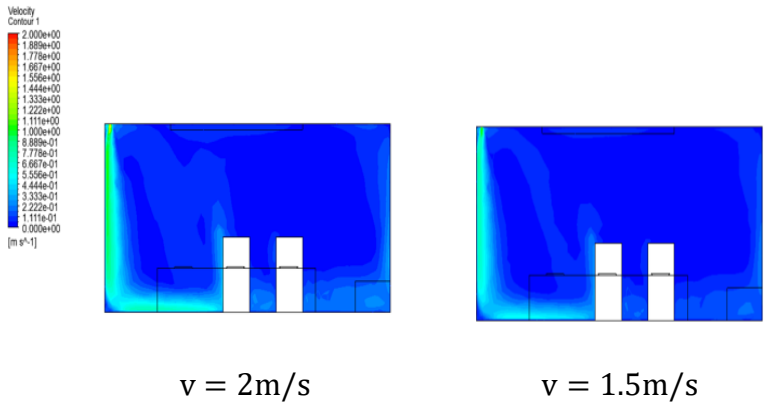

$v = 2m/s$ $v = 1.5m/s$

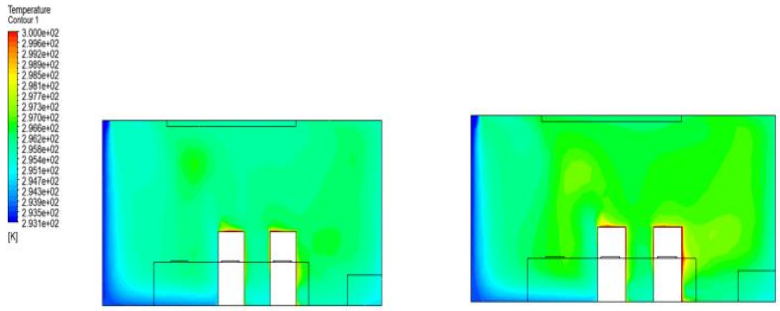

$v = 2m/s$ $v = 1.5m/s$

Figure 32

From case 1.2 and case 2.2, it can be seen that when the characteristic cross section is close to the air outlet. When the obstruction of the airflow attached to the ground is removed, flow field becomes well-uniform, distribution of the airflow field does not change with the reduction of the delivery speed and remains stable. When temperature is maintained at 23℃, temperature difference can be maintained within 1℃ to 2℃ by reducing the air supply speed.

$Case\ 3.2\ x = 1.95m$

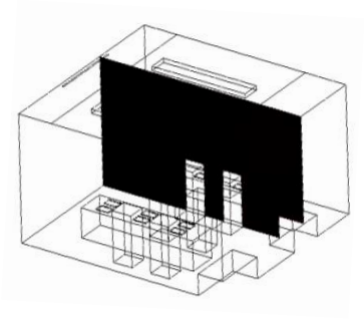

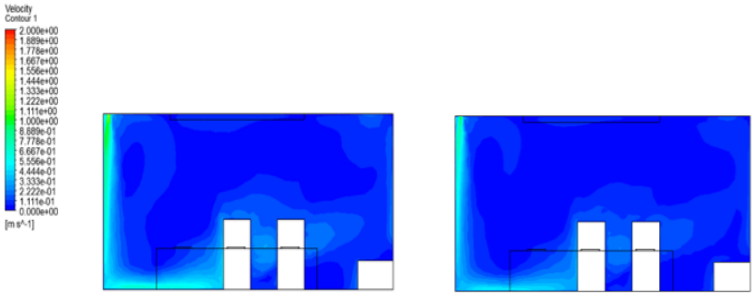

$v = 2m/s$ $v = 1.5m/s$

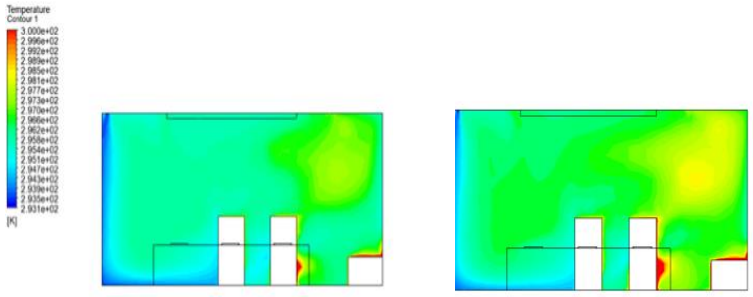

$v = 2m/s$ $v = 1.5m/s$

Figure 33

Case 4.2 $x = 1.5m$

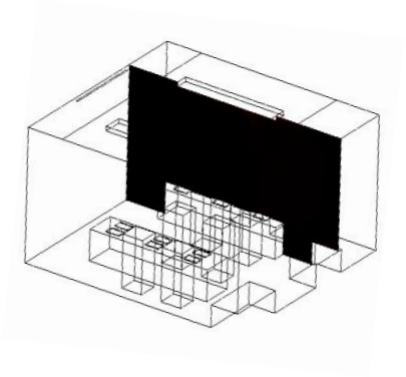

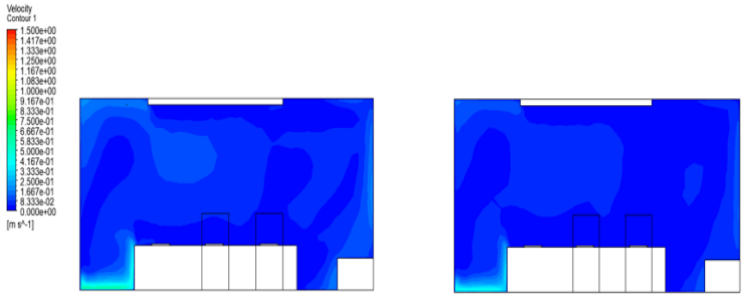

$v = 2m/s$ $v = 1.5m/s$

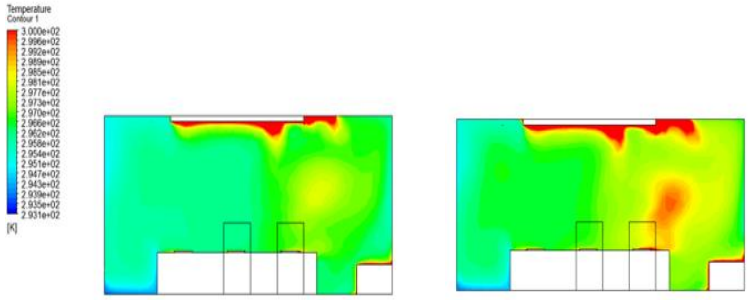

$v = 2m/s$ $v = 1.5m/s$

Figure 34

As can be seen from case 3.2 and case 4.2, during the gradual movement of the characteristic cross-section away from the air conditioning outlet, there is no large-scale high-temperature clustering in the indoor temperature field, and the temperature distribution is more uniform from an overall perspective. From the temperature contour it can be seen that the high temperature trends all appear in the back half of the room, with the highest temperature of 26℃.

From the velocity field, when the characteristic section is far away from the air

conditioning outlet, the velocity field begins to appear stratification phenomenon, but the velocity difference is almost maintained at 0.1m/s. In this way, the indoor personnel will not have obvious blowing sensation, but also can help improve the ventilation efficiency.

Case 5.2 $x = 0.35$

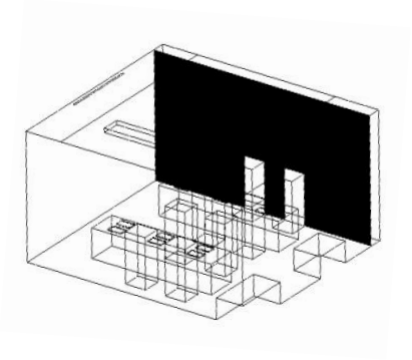

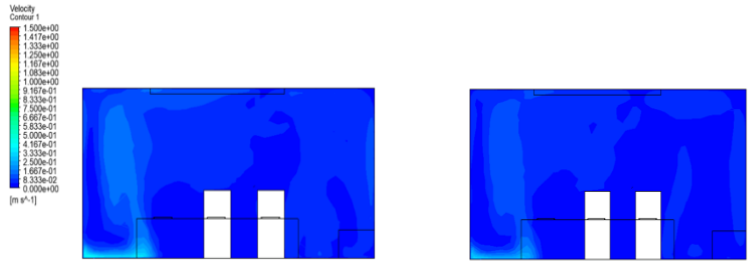

$\mathrm{v} = 2\mathrm{m/s}$ $\mathrm{v} = 1.5\mathrm{m/s}$

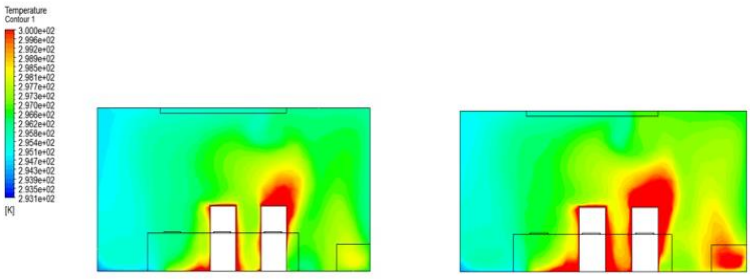

$\mathrm{v} = 2\mathrm{m/s}$ $\mathrm{v} = 1.5\mathrm{m/s}$

Figure 35

Case 5.2 is the farthest cross-section from the air supply, because the personnel as heat sources, dissipate heat outward, therefore, the temperature around the human body is higher than the surrounding ambient temperature, the highest temperature reaches 27℃. From the human body heat dissipation on the surrounding environment, the heat aggregation group mainly appears in the vicinity of the heat source, and does not

produce vortex phenomenon, the airflow distribution is more uniform. The average temperature here is higher due to the limited inertial force of airflow adhering along the ground, which cannot reach further areas. Compared with other cases, the air conditioning air supply speed has an impact on the distribution of the airflow field, and when the air supply speed is not large enough, it will aggravate the generation of the heat aggregation phenomenon.

5.4 Summary

With the reduction of indoor personnel, the air supply body mixes more fully with the indoor air, and the room velocity and temperature parameters are more uniform. With the reduction of obstructions, the development section of the attached jet is formed more fully, and at this time, the vertical wall attached ventilation air supply form has a higher energy utilization rate. Moreover, when the attached jet development section is sufficiently developed, except for the working condition 5.2 that is far away from the air conditioning air supply, other working conditions show that the air supply velocity has no great influence on the distribution of the flow field.

Chapter 6: Thermal comfort analysis

Selected six indoor personnel, according to their location from the air conditioning outlet at different distances, numbered 1 to 6, as shown in the figure36, which represent the closest to the air outlet front row of personnel for the number 2, 3, 6. Where the No. 6 compared to the other two personnel away from the air outlet; No. 4 and No. 5 represent in the core area of the heat source; No. 1 from the air outlet furthest away.

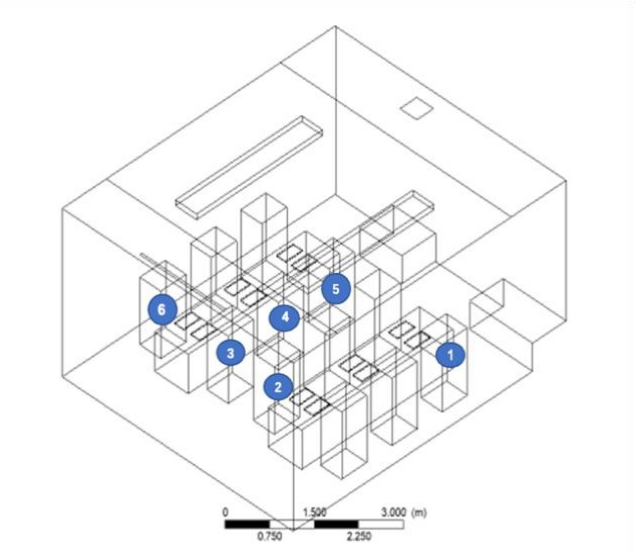

Figure 36

6.1 Effect of air supply speed on thermal comfort under the condition of the dense heat sources

By comparing the PMV and PDD indexes of the office personnel numbered 1 to 6, it can be seen from figure 37：

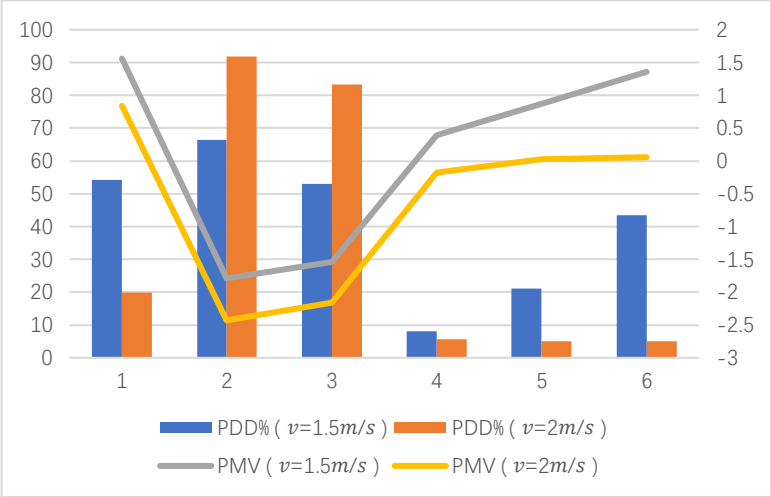

Figure 37

Among the front row personnel, No. 2 and No. 3 are close to the air outlet and feel too cold no matter which wind speed they are in. No. 6, who is also a front-row person, can keep a comfortable state with PDD<10% when the air supply speed V=2m/s，because it is far from the air outlet; No. 1, who is far from the air outlet, also needs to be at a larger wind speed to satisfy the comfort, otherwise it will produce a stifling feeling. No. 4 and No. 5, which are at the center of the heat source, basically meet the comfort level regardless of the wind speed.

When the speed was reduced to 1.5m/s. Only No. 4 felt comfortable. the PMV value as a whole shifted upward, indicating enhanced heat sensation. As the personnel near the air outlet feel cold and the personnel at the far end of the air outlet feel stuffy and hot， it indicates that there is uneven heat and cold in the room under this condition, the cooling effect is poor, and the cold air cannot fill the whole room uniformly.

6.2 Comparative analysis of thermal comfort under different heat source conditions

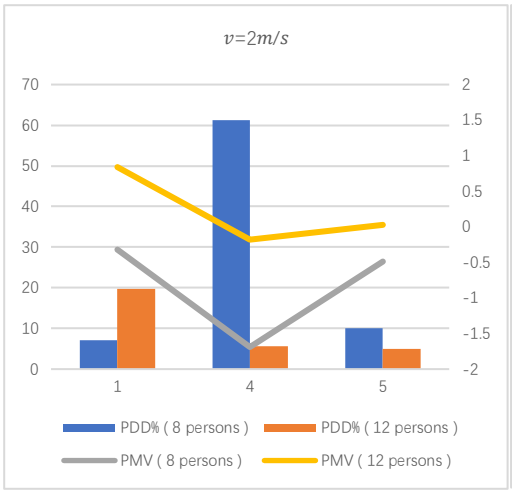

Figure 38

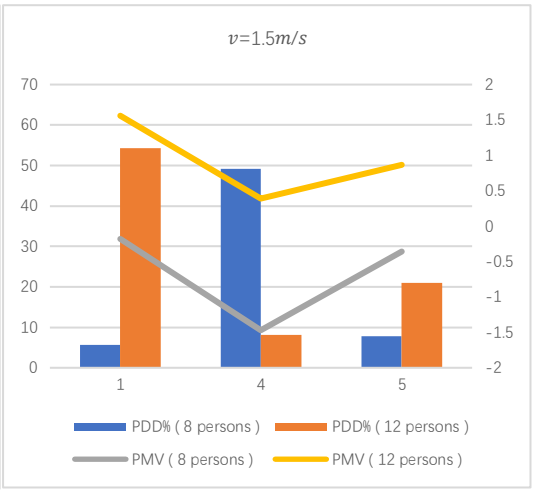

Figure 39

From Figure 38 and Figure 39, feeling of coldness in the room is strong, satisfaction level is low. In the case of less people in the room (less heat sources), the temperature should be increased by appropriate air supply temperature.

When applying strong and dense eat source (12 persons), the air supply speed has a greater effect on the indoor temperature field: the reduction in air supply speed leads to an increase in PMV, enhanced thermal sensation, and a significant increase in PDD. However, after reducing the indoor heat source (8 persons), the air supply speed has little effect on the indoor thermal environment, which corresponds to the conclusion reached in the previous chapter: under the same conditions of air supply temperature and air supply speed, when reducing the obscuration of the ground-attached airflow while reducing the heat source, the overall indoor temperature is significantly declined, and the change of air supply speed has little effect on the indoor temperature, and still maintains a better cooling effect.

Chapter 7: Conclusions and recommendations

In this study, a literature survey was conducted for a new ventilation method based on vertical wall-attached jet: air curtain jet (ACJ) ventilation [21], which shows that the new ventilation is a highly efficient ventilation method combining the advantages of traditional ventilation methods, and that it can satisfy the thermal comfort. However, effect of the new ventilation applied to different heat loads has been little studied.

CFD was used to study the characteristics of airflow field distribution at different air supply velocities. Coanda effect was successfully simulated, which once again proved the feasibility of using the SST k-ω model to simulate the vertical wall apposed ventilation. By setting the characteristic cross-section, the result plots of the airflow temperature and velocity fields at different supply air velocities were obtained, and it was concluded that:

1. The difference in the air flow field distribution is strongly related to the distance from the air supply outlet. If the airflow is blocked at the stage of adhering to the floor, so that it is not sufficiently developed, the cold air cannot spread to a greater distance, resulting in uneven flow field, the cooling effect is decreased.

2. Velocity and temperature fields are comparatively analyzed, found that it is necessary to keep a large air supply velocity to maintain the cooling effect in the room when crowded with people.

Then, as a comparison, the reduced heat source condition was simulated by designing the condition with reduced front row personnel. In this study, the airflow traces, temperature field, and velocity field under different heat source conditions were compared and analyzed, represented by the air supply velocity v=2m/s. After that, the airflow field distribution under the reduced heat source condition was also compared and analyzed for the reduced heat source condition, and it was concluded that:

1. A comparative study of reducing front row personnel shows that the effectiveness of the new vertical wall attachment ventilation method is highly dependent on personnel distribution and equipment placement. The density of

personnel in the room has a significant impact on the indoor air flow field. The overall temperature in the work area is significantly reduced with fewer personnel, due to the removal of the obstruction to the floor-attached air supply, which allows the airflow to spread more, allowing for better heat exchange with the heat source and better cooling of the room by the cool air.

2. When the indoor heat load is large and the heat source is dense, in order to need to ensure the diffusion of the air supply floor attached to the air supply, the wind speed in the design should not be too small when using the new vertical wall attached ventilation method, it is recommended that the wind speed is not less than 1.5 m / s. However, due to the large wind speed, personnel near the air outlet will feel cold. The cooling effect will be significantly decreased when the floor air supply airflow is obstructed. Therefore, it is recommended that the horizontal distance of 1 to 2m from the air conditioning outlet is appropriately reserved space, and no personnel are arranged, or no items are set up for placement to ensure the transmission of cool air and the comfort of personnel.

Finally, the indoor thermal comfort under different wind speed and different heat source conditions was studied and compared, and it was concluded that: effect of air supply velocity on the indoor temperature when the indoor heat source is strong and dense.

This result also verifies the previous conclusions that under the same conditions of air supply temperature and air supply speed, the overall indoor temperature decreases significantly with the reduction of the heat source while reducing the shading of the airflow attached to the ground, and the change of air supply speed has little effect on the indoor temperature and still maintains a better cooling effect.

Chapter 8: Proposal for further works

In this study, for the airflow characteristics of the room using the new vertical wall attached ventilation method, this paper uses the CFD numerical method to simulate velocity and temperature. Through comparative analysis, the results of the factors influencing the room airflow field and the comfort of indoor personnel are obtained. Due to time and conditions, there are many areas that are not fully satisfactory, and the following issues will be improved in future research studies.

1. due to the differences of individual personnel, it should be more subdivided to discuss the human comfort of different genders and different ages.

2. The human body model treatment in this study became rectangular, and the model should be further refined in future studies.

3. The conclusions of this paper rely only on numerical simulations, and in future studies, full-scale experiments should be established for further validation.

References

[1] Kreiss K. (1989). The epidemiology of building-related complaints and illness. Occupational medicine (Philadelphia, Pa.), 4(4), 575–592.

[2] Singh, J. (1996). Review: Health, Comfort and Productivity in the Indoor Environment. Indoor and Built Environment, 5, 22 - 33.

[3] Clausen, G., Fernandes, E. O., De Gids, W. and Delmotte, C. (2003) ECA Report No 23: Ventilation, Good Indoor Air Quality and Rational Use of Energy. Luxembourg: European Commission.

[4] Buonomano, A., Sherman, M., 2009. Analysis of residential hybrid ventilation performance in US climates, in: Proceedings of the AIVC 30th Conference: Trends in High Performance Buildings and the Role of Ventilation. pp. 1–2.

[5] Cao, Guangyu & Awbi, H.B & Yao, Runming & Fan, Yunqing & Sirén, Kai & Kosonen, R. & Zhang, Jianshun. (2014). A review of the performance of different ventilation and airflow distribution systems in buildings. Building and Environment. 73. 171-186. 10.1016/j.buildenv.2013.12.009.

[6] Shah, Mona & Deshpande, Rahul & Jadhav, Tushar. (2017). Alternatives to conventional air conditioning systems – A review.

[7] Yin, Haiguo & Li, Angui. (2012). Airflow characteristics by air curtain jets in full-scale room. Journal of Central South University. 19. 10.1007/s11771-012-1056-8.

[8] Cao, Guangyu & Awbi, H.B & Yao, Runming & Fan, Yunqing & Sirén, Kai & Kosonen, R. & Zhang, Jianshun. (2014). A review of the performance of different ventilation and airflow distribution systems in buildings. Building and Environment. 73. 171-186. 10.1016/j.buildenv.2013.12.009.

[9] Chitaru, G., Berville, C., & Dogeanu, A. (2018). Numerical simulation and comparison of two ventilation methods for a restaurant – displacement vs mixed flow ventilation.

[10] Chau, Hing-Wah & Zhou, Jin & Kang, Ye & Hes, Dominique & Noguchi, Masa & Aye, Lu. (2018). Comparing Mixing Ventilation and Displacement Ventilation in

University Classrooms.

[11] Melikov, A. (2016). Advanced air distribution: improving health and comfort while reducing energy use. Indoor air, 26 1, 112-24.

[12] Brunk, M.F. (1993). Cooling ceiling-an opportunity to reduce energy costs by way of radiant cooling. ASHRAE Transactions. 99. 479-487.

[13] ASHRAE: (2001) “Handbook of Fundamentals”, American Society of Heating, Refrigeration and Air- Conditioning Engineers, Atlanta GA.

[14] Goodfellow, H. D., 2001. Industrial Ventilation Design Guidebook. Academic Press, Chapter 11.

[15] Nielsen, P. V. (2000). Velocity Distribution in a Room Ventilated by Displacement Ventilation and Wall-Mounted Air Terminal Devices. Energy and Buildings, 31(3), 179-187.

[16] Seppänen, O. (2007). Ventilation strategies for good indoor air quality and energy efficiency. International Journal of Ventilation, 6, 297-306.

[17] Chitaru, G., Berville, C., & Dogeanu, A. (2018). Numerical simulation and comparison of two ventilation methods for a restaurant – displacement vs mixed flow ventilation.

[18] Awbi, H.B. (1998). Energy efficient room air distribution. Renewable Energy. 15. 293-299. 10.1016/S0960-1481(98)00176-1.

[19] Goodfellow, H. D., 2001. Industrial Ventilation Design Guidebook. Academic Press, Chapter 11.

[20] Awbi, H.B. (2003). Ventilation of Buildings (2nd ed.). Routledge. https://doi.org/10.4324/9780203634479

[21] Yin, H., & Li, A. (2012). Airflow characteristics by air curtain jets in full-scale room. Journal of Central South University, 19, 675-681.

[22] Coanda, H., US Patent # 2,052,869, Device for Deflecting a Stream of Elastic Fluid Projected into an Elastic Fluid, 1936.

[23] Boscoianu, M., Prisecariu, V., & Cîrciu, I. (2010). APPLICATIONS AND COMPUTATIONAL ASPECTS REGARDING THE COANDĂ EFFECT.

[24] Li, A., Yi, H., & Zhang, W. (2012). A Novel Air Distribution Method -

Principles of Air Curtain Ventilation. International Journal of Ventilation, 10, 383 - 390.

[25] Tu, C.V., & Wood, D.H. (1996). Wall pressure and shear stress measurements beneath an impinging jet. Experimental Thermal and Fluid Science, 13, 364-373.

[26] Yuan, X.Y., Chen, Q., Glicksman, L., Hu, Y., & Yang, X. (1999). Measurements and computations of room airflow with displacement ventilation.

[27] Liu WX (2016). Study on the effects of indoor heat source and the obstacle by Air Curtain Ventilation. Master Thesis, Xi'an university of Architecture and Technology, China. (in Chinese)

[28] Boscoianu, Mircea & Prisacariu, Vasile & Circiu, Ionica. (2010). Applications and computational aspects regarding the Coandă effect. SCIENCE & MILITARY.

[29] Li, A. (2019). Extended Coanda Effect and attachment ventilation. Indoor and Built Environment, 28(4), 437–442.

[30] Xue, H. & Shu, Chang. (1998). Mixing characteristics in a ventilated room with non-isothermal ceiling air supply. Building and Environment. 34. 245-251. 10.1016/S0360-1323(98)00015-8.

[31] CRAFT, T. & Launder, Brian. (2001). On the Spreading Mechanism of the Three-Dimensional Turbulent Wall Jet. Journal of Fluid Mechanics. 435. 305 - 326. 10.1017/S0022112001003846.

[32] Cho, Y. & Awbi, H.B & Karimipanah, Taghi. (2008). Theoretical and experimental investigation of wall confluent jets ventilation and comparison with wall displacement ventilation. Building and Environment. 43. 1091-1100. 10.1016/j.buildenv.2007.02.006.

[33] Zhang WD (2002). Prediction and visualizing validation of downward directed vertical wall jets and air lake phenomena. Master Thesis, Xi'an university of Architecture and Technology, China. (in Chinese)

[34] Yin, H (2012). Study on design procedures of air distribution by air curtain ventilation with a linear slot diffuser. PhD Thesis, Xi'an University of Architecture and Technology, China. (in Chinese)

[35] Wang RL (2015). Study of velocity and temperature field of non-isothermal attached air curtain ventilation mode. Master Thesis, Xi'an university of Architecture

and Technology, China. (in Chinese)

[36] He XJ（2020）.Study on the air distribution performance of vertical wall attached ventilation, displacement and mixing ventilation. Master Thesis, Xi'an university of Architecture and Technology, China. (in Chinese)

[37] Jones, P.J., & Whittle, G.E. (1992). Computational fluid dynamics for building air flow prediction—current status and capabilities. Building and Environment, 27, 321-338.）

[38] Ismail-Zadeh, A. & Tackley, P.J. (2010). Computational methods for geodynamics. Computational Methods for Geodynamics. 1-330. 10.1017/CBO9780511780820.

[39] Nielsen, P. V., Restivo, A., & Whitelaw, J. H. (1978). The Velocity Characteristics of Ventilated Rooms. Journal of Fluids Engineering - Trancactions of The ASME, 100(3), 291-298.

[40] Ashrae, A. N. S. I. (2013). Standard 55-2013: Thermal Environmental Conditions for Human Occupancy. American Society of Heating, Refrigerating, and Air-Conditioning Engineers, Inc. Atlanta.

[41] Fanger, P. O. (1970). Thermal comfort. Analysis and applications in environmental engineering. Thermal comfort. Analysis and applications in environmental engineering.

[42] Castro, F., Palma, J., & Silva Lopes, A. (2004). Simulation of the Askervein Flow. Part 1: Reynolds Averaged Navier–Stokes Equations (k∈ Turbulence Model). Boundary-Layer Meteorology, 107(3), 501-530.

[43] Wilcox, D.C. (1993). Turbulence modeling for CFD.

[44] Bradshaw, P.M. (1998). Fundamentals of Turbulence Modeling. By C.-J. Chen & S.-Y. Jaw. Taylor and Francis, 1998. xii+292 pp. ISBN 1-56032-405-8. £34.95. Journal of Fluid Mechanics, 371, 379-381.

[45] Liu WX (2016). Study on the effects of indoor heat source and the obstacle by Air Curtain Ventilation. Master Thesis, Xi'an university of Architecture and Technology, China. (in Chinese)

[46] Yin, H., & Li, A. (2016). Study of attached air curtain ventilation within a full-

scale enclosure: comparison of four turbulence models. Indoor and Built Environment, 25(6), 962–975.